Bioresource Technology 300 (2020) 122700

Contents lists available at ScienceDirect

Bioresource Technology

journal homepage: www.elsevier.com/locate/biortech

Assessing thermal behaviours of cellulose and poly(methyl methacrylate) during co-pyrolysis based on an unified thermoanalytical study

Gamzenur Özsin

Bilecik Şeyh Edebali University, Faculty of Engineering, Department of Chemical Engineering, Bilecik, Turkey

ARTICLE INFO

Keywords:
Cellulose
PMMA
Co-pyrolysis
Kinetic parameters
Thermogravimetry

ABSTRACT

The objective of this study was to evaluate pyrolysis and co-pyrolysis behavior of cellulose and poly(methyl methacrylate) (PMMA) and examine the kinetics of the processes by using thermogravimetric analysis (TGA) coupled with FT-IR spectrometry. For this purpose, non-isothermal experiments were carried out using different heating rates and three prominent iso-conversional methods were used to obtain kinetic parameters at various extents of conversions from 0.1 to 0.9. Blending PMMA with cellulose had a marked effect on the process. The results of co-pyrolysis using a blending ratio of 50 wt% PMMA indicated that the highest rate of pyrolytic transformation was achieved at a conversion degree of 0.5 while activation energy ranged from 188.1 to 364.3 kJ/mol. The most intensive gas release during cellulose pyrolysis was CO_2. Co-pyrolysis was more complicated than that of pyrolysis of cellulose and PMMA due to depolymerization and radical interactions.

1. Introduction

Solid wastes like plastics have become a primary concern of global waste treatment since they are widely produced as a result of their extensive application areas. On the other hand, population growth, industrialization, and increasing urbanization rates necessitate sustainable and environmentally-friendly energy resources which may substitute fossil fuels which are limited and deplete rapidly (Jin et al., 2017; Singhania et al., 2013). Therefore, waste management authorities have shifted their strategies towards waste to energy (WtE) processes. The ultimate goal of these processes is to replace polluting, non-renewable energies with sustainable energy resources (Cherpozat et al., 2019). At this point, thermochemical conversion methods are attractive options because they can notably reduce and eliminate waste volumes together with diversifying energy resources and mitigating the environmental impacts related to fossil fuels (Awasthi et al., 2019; Chen et al., 2019; Sharifzadeh et al., 2015).

Among major thermochemical processes, pyrolysis has been considered to be the most cost-effective, producing value-added fuels and chemicals (Bartocci et al., 2018; Ding et al., 2018). It offers several advantages such as product feedstock versatility, uniformity, scalability and high efficiency in comparison to other chemical and biochemical conversion techniques (Déparrois et al., 2019). To produce high-grade fuels and chemicals from more than two distinct materials as precursors, another improved technique of pyrolysis is used, and it is known as co-pyrolysis (Jin et al., 2019). In particular, co-pyrolysis of biomass and polymers is a promising process since using polymeric structures donates in-situ hydrogen during the biomass pyrolysis process and causes radical interactions that may cause synergetic effects and reduction of activation energy (Kumari & Singh, 2019; Li et al., 2013; Patil et al., 2018; Xiang et al., 2018).

The pyrolysis mechanisms during biomass decomposition are closely related to the quantity and form of three major components as cellulose, hemicellulose, and lignin. Therefore, several studies on singular components of lignocellulosic biomass have been performed to explain the pyrolysis characteristics of cellulose, hemicellulose and lignin individually, as well as their interactions in the lignocellulosic matrix, (Burhenne et al., 2013; Collard & Blin, 2014; Giudicianni et al., 2013; Qu et al., 2011; Stefanidis et al., 2014; Yang et al., 2007; Yang et al., 2006; Zhang et al., 2015; Zhao et al., 2017; Zhou et al., 2015) while some other studies have focused on the co-pyrolytic behaviors of these three components to gain information about the interactions among biopolymer and synthetic polymer structures. This is because the biochemical composition of biomass has a marked effect on the co-pyrolysis process since the process involves the formation of intermediates and solid, liquid and gaseous products through multiphase complex reactions of competing coupled pathways (Bu et al., 2019). Therefore, product yields and characteristics are determined by not only process conditions (like temperature, heating rate, pressure, residence time and catalysis by indigenous inorganics) but also the nature and intrinsic composition of raw materials (Shafaghat et al., 2019). For these reasons, the physicochemical properties and thermal

E-mail addresses: gozsin@anadolu.edu.tr, gamzenur.ozsin@bilecik.edu.tr.

https://doi.org/10.1016/j.biortech.2019.122700
Received 23 December 2019; Accepted 24 December 2019
Available online 27 December 2019
0960-8524/

decomposition behaviors of precursors should be fully understood before design and operation of co-pyrolysis reactors and plants.

In the organic fraction of biomass, there are three main biopolymers as cellulose, hemicellulose, and lignin, and their relative compositions vary significantly in the biomass species. Furthermore, the relative roles of these three components in pyrolysis and co-pyrolysis processes have not been defined well yet (Debiagi et al., 2016). Several studies have already been reported about the various aspects of co-pyrolysis with polymeric structures together with cellulose, hemicellulose, and lignin. However, the distinctive properties of each polymer make it impossible to achieve a consensus on precise polymer-biopolymer interactions during co-pyrolysis. Since the radical interactions during co-pyrolysis are critical issues for bio-refineries, cellulose/PMMA co-pyrolysis was investigated in deepening the understanding of the thermokinetics of the process in this study. Previous attempts have been put forth to shed light on co-pyrolysis of cellulose with polypropylene, polyethylene, polystyrene, polyvinyl chloride, and polyvinylidene chloride (Matsuzawa et al., 2001; Suriapparao et al., 2014) to understand the multiphase complexities of co-pyrolysis with cellulose. However, interactions of PMMA with cellulose and the kinetics of the process have never been investigated during co-pyrolysis. The contribution of this paper is to be the first study in the literature that focuses on co-pyrolysis of PMMA and cellulose which is based on TGA/FT-IR study.

2. Materials and methods

2.1. Non-isothermal TGA/FT-IR experiments

Cellulose and PMMA were all obtained from Sigma-Aldrich. Prior to the experiments elemental analysis of raw materials was conducted by an elemental analyzer (Leco-CHNO). The acquired elemental analysis results are given in Table 1. A Cellulose/PMMA blend was prepared by homogenously mixing cellulose and PMMA powders with a 50 wt% mass ratio in an agate mortar for investigation. Also, samples with 25 wt% of PMMA was blended to understand the effect of blending ratio on thermokinetics of co-pyrolysis process by comparing the results of 50 wt% of PMMA.

Pyrolysis and co-pyrolysis runs were carried out in a TGA device (Setaram-Labsys Evo) which was coupled with an FT-IR spectrometer (Thermo Scientific iz10). In order to explore thermal events, a continuous nitrogen flow was maintained (with a flow rate of 20 cm^3/min). A small amount of a sample (approximately 10 mg) was weighted precisely to eliminate systematic errors and minimize the mass and heat transfer limitation. After placing the sample onto the alumina pan of the device, the temperature was raised from 25 to 1000 °C using linear heating rates from 5 to 40 °C/min. Prior to the online experiments, blank experiments were performed to obtain the baselines to be used as corrections. The transfer line and the spectrometer cell were firstly preheated to avoid condensation of the products which were quickly carried by the N_2 stream to the spectrometer chamber for detection during the pyrolysis and co-pyrolysis processes. The gases evolved from TGA during pyrolysis and co-pyrolysis were identified by collecting simultaneous FT-IR spectra. The background data were collected prior to collecting the FT-IR spectra. A total of 32 spectral lines with 4 cm^{-1} resolutions were acquired in the range 4000–400 cm^{-1} IR absorption band. All the experiments were carried out at least three times to satisfy the reproducibility criterion. Analysis of instantaneous and 3D spectra was carried out by the help of the OMNIC software.

Table 1
Elemental analysis results of cellulose and PMMA (as-received basis).

	Cellulose	PMMA
C (wt. %)	42.38	59.22
H (wt. %)	6.06	7.20
N (wt. %)	<0.10	<0.10
O* (wt. %)	51.56	33.58
H/C	1.70	1.45
O/C	0.91	0.42

* From difference.

2.2. Calculation of kinetic parameters

TGA is a well-established analytical technique in determination of the reaction kinetics of pyrolysis which is related to the weight loss characteristics of the precursor. By the help of simultaneous recording of the weight loss as the temperature is increasing at a uniform rate during non-isothermal runs, a kinetic triplet can be obtained. Non-isothermal TGA data may provide information about kinetic parameters by applying both model-free and model-fitting methods. Bearing in mind that pyrolysis includes a series of heterogeneous reactions, model-fitting methods necessitate preselection of the order of reactions, mechanisms and kinetic equations (Tahir et al., 2019). On the contrary, model-free methods enable estimation of kinetic parameters without an explicit model and eliminate systematic errors at different heating rates (Tahir et al., 2019; Yan et al., 2019). Because numerous heterogeneous reactions take place simultaneously along with mass, momentum and heat transfer within the heterogeneous fuel matrix, a precise modeling of the pyrolysis reaction pathways is nearly impossible (Amini et al., 2019; Ashraf et al., 2019).

The basis of TGA-based kinetics is derivation of the conversion degree (α) from the mass loss in the sample mass as a function of temperature or time which is calculated based on the following equation:

$$\alpha = \frac{w_o - w_t}{w_o - w_f} \tag{1}$$

where; w_t is the sample mass at time t or temperature T, and w_o and w_f are the sample masses at the beginning and at the end of the reaction, respectively. On the other hand, the pyrolysis reactivity index (R_p) may be calculated with the following formula:

$$R_p = \frac{1}{w_o}\left(\frac{dw}{dt}\right)_{max} \tag{2}$$

where $(dw/dt)_{max}$ is the maximum pyrolysis rate and w_o is the initial weight before the pyrolysis stage. A general expression for non-isothermal methods with a constant heating rate (β = dT/dt) kinetic expression is defined by two different functions, namely the temperature function (k(T)) and the fractional conversion function (f(α)), as given in Eq. (3):

$$\frac{d\alpha}{dt} = \beta\frac{d\alpha}{dT} = k(T)f(\alpha) \tag{3}$$

Since the Arrhenius equation expresses temperature dependency by a calculation of the rate constant, k; [k = Aexp(-E_a/RT)] (where E_a is the activation energy, A is the pre-exponential factor and R is the gas constant), the reaction rate equation may be modified as shown in Eq. (4):

$$\beta\frac{d\alpha}{dT} = A\exp\left(-\frac{E_a}{RT}\right)f(\alpha) \tag{4}$$

Integration of both sides of Eq. (4) gives:

$$\int_0^\alpha \frac{d\alpha}{f(\alpha)} = g(\alpha) = \frac{A}{\beta}\int_{To}^{T}\exp\left(-\frac{E_a}{RT}\right)dT \tag{5}$$

where g(α) is the function of the integrated form of conversion degree. The kinetic model f(α) is associated with a physical model which describes the kinetics. In order to predict the activation energy with respect to the conversion degree three different iso-conversional models were applied to the experimental data within the scope of this study. The most remarkable advantage of such methods is their satisfactory suitability for more complex and multiple-step reactions (Bedoić et al.,

2019). The basis of these iso-conversional methods is that the rate is calculated by the current sample temperature at a certain extent of conversion, and heating rate and temperature changes are considered as ineffective on the reaction mechanism (Xiang et al., 2018). Therefore, Eq. (6) is valid for the iso-conversional principle:

$$\left[\frac{d\ln(d\alpha/dt)}{dT^{-1}}\right]_{\alpha} = -\frac{E_{\alpha}}{R} \tag{6}$$

In order perform kinetic analysis by the iso-conversional approach, a series of experiments at different heating rates has to be performed. The linearized forms of the kinetic methods used in this study, namely Friedman, FWO and KAS, are given in Eqs. (7), 8 and 9, respectively.

$$\ln\left(\beta\frac{d\alpha}{dT}\right) = \ln A + \ln f(\alpha) - \frac{E_a}{RT} \tag{7}$$

$$\ln\beta = \ln\frac{AE_a}{Rg(\alpha)} - 5.331 - 1.052\frac{E_a}{RT} \tag{8}$$

$$\ln\left(\frac{\beta}{T^2}\right) = \ln\left(\frac{AR}{E_a g(\alpha)}\right) - \frac{E_a}{RT} \tag{9}$$

In order to estimate the pre-exponential factor (A_α) values for each conversion degree, Kissinger's equation as given in Eq. (10) is used:

$$A_{\alpha} = \frac{\beta E_{\alpha}\exp(E_{\alpha}/RT_m)}{RT_m{}^2} \tag{10}$$

where T_m is the temperature at the maximum conversion rate.

2.3. Characterization of carbonaceous intermediates and cellulose char

The physical and characteristics of solid residues at different temperature stages were analyzed using SEM-EDX and FT-IR spectroscopy techniques. Before the SEM-EDX analysis, samples were coated with Au and Pd using a sputter coater to minimize sample charging. Micrographs were taken using an accelerating voltage of 20 kV at several magnifications using Zeiss Supra VP40. FT-IR spectra of the samples were obtained in absorbance mode with a wavenumber range of 4000–400 cm^{-1} using Perkin Elmer Spectrum 100 spectrometer.

3. Results and discussion

3.1. Thermogravimetric analysis

Multiple pyrolysis and co-pyrolysis characteristics of cellulose and PMMA at heating rates of 5, 10, 20 and 40 °C/min are illustrated by the help of the mass loss and derivative mass loss curves which are given in Figs. 1 and 2 to reveal the mechanisms. Moreover, Table 2 summarizes the general pyrolytic and co-pyrolytic characteristics of the cellulose and PMMA quantitatively. From the perspective of the characteristics of cellulose in pyrolysis, which started at approximately 263 °C and ended at 455 °C, the maximum weight loss was observed near 330 °C. A single dTG peak indicated that pyrolytic decomposition occurred at a single stage which included evolution of condensable organic compounds. The solid residues were about 21 wt% of the initial weight of the sample for the active pyrolysis region. With the increase in temperature after this main decomposition zone, the mass loss rate changed slowly and reached an asymptotic value near 15 wt% of the initial value during the charring process. Based on previous studies, the passive pyrolysis region of cellulose includes rearrangement in a polycyclic structure and conversion of short substituent groups of the aromatic rings (Collard & Blin, 2014). Depending on the applied heating rate, the characteristic pyrolysis temperatures were changed as it may be observed in Table 2. The reactivity of cellulose increased from 1.30 to 7.31 when the heating rate was changed from 5 to 40 °C.

The temperature range of active pyrolysis for PMMA was recorded between 239 °C and 477 °C. The pyrolysis interval of PMMA could be divided into two stages which consisted of degradation by end chain scission (Wilkie, 1999). Thermal degradation of PMMA is known to be initiated by radical transfer to the unsaturated chain end which is then followed by homolytic scission of the chain due to head-to-head bonds, radical transfer to the unsaturated chain end and random scission of the chain (Laachachi et al., 2004). It may be noticed that the heating rate had a marked effect on the samples by shifting the TG and dTG curves to higher temperatures. Besides, the reactivity of PMMA was found to increase from 0.49 to 3.38%/min.mg depending on the heating rate. Approximately 65 wt% of the initial weight remained after the first stage of PMMA degradation. Depending on the heating rate, the maximum mass loss rate occurred at 297.14, 284.02, 288.44 and 291.55 °C. The mass loss at the second stage led to the full degradation of the structure, and the mass loss approached to zero.

The co-pyrolysis process of cellulose and PMMA (50 wt% cellulose /50 wt.%PMMA) exhibited a stepwise decomposition as expected, and the active pyrolysis zone of co-pyrolysis could be divided into three steps. During the initial stage, the lowest weight loss of the blend occurred as approximately 10 wt% up to 330 °C. The second weight loss was about 45 wt% which had a relatively higher mass loss rate than the other steps. Above this second stage, the mass change rate changed slowly during the final, third stage until the final temperatures are between 436.81 and 468.27 °C. The final residual masses after the active co-pyrolysis region were between 14.44 and 13.04. wt. % depending on the heating rate. The reactivity values of co-pyrolysis changed from 0.76 to 5.39 due to increasing heating rate from 5 to 40 °C/min. Based on the initial and final temperatures together with peak temperatures during the pyrolysis and co-pyrolysis processes of all samples, a shifting to higher temperatures by increasing the heating rate was observed due to the hysteresis effect. However, the TG and dTG profiles remained nearly the same, which indicated that similar reaction mechanisms occurred at all heating rates. When co-pyrolysis was performed by using 25 wt% of PMMA obtained results showed that increasing cellulose content during co-pyrolysis increased reactivity values for all of the heating rates. This observation may have implied that more radical reactions were triggered by using high cellulose content. Also the second peak at active co-pyrolysis region disappeared due to overlapping from TG and dTG thermograms.

To further study the interactions of cellulose and PMMA during co-pyrolysis, dTG peak deconvolution was used for the co-pyrolysis process (for 50 wt.%/cellulose/50 wt% PMMA). As deconvolution is an effective mathematical method, it is utilized to separate the overlapped dTG peaks of co-pyrolysis to observe distinct peaks and gain information on these separated peaks. The normalized dTG curve as a function of temperature was deconvoluted into Gaussian distributions by using the Peak Analyzer tool of the Origin Pro software. By comparing the experimental dTG curves to the deconvoluted curves, determination of interactions between cellulose and PMMA may be possible. The deconvoluted dTG curves obtained at different heating rates are given in Fig. 3. Accordingly, the curves were perfectly fitted by the Gaussian type function, and the deconvolution procedure evidenced three distinct peaks during the co-pyrolysis process for all of the heating rates that were applied. The amount of deconvoluted peaks was independent of the applied heating rate, and the percentage error of the fitted curves with respect to the experimental curves was below 2%. Comparison between the co-pyrolysis experimental dTG curves and deconvoluted dTG showed that the co-pyrolysis peak temperatures were slightly different than the peak temperatures of the individual components which may indicate synergetic effects between cellulose and PMMA during active pyrolysis stage.

3.2. Evaluation of pyrolysis and co-pyrolysis kinetics

For the determination of the activation energy, the conversion degree from 0.1 to 0.9 was taken into account and the results are given in Table 3 and Fig. 4. The minimum energy amount needed to initiate a

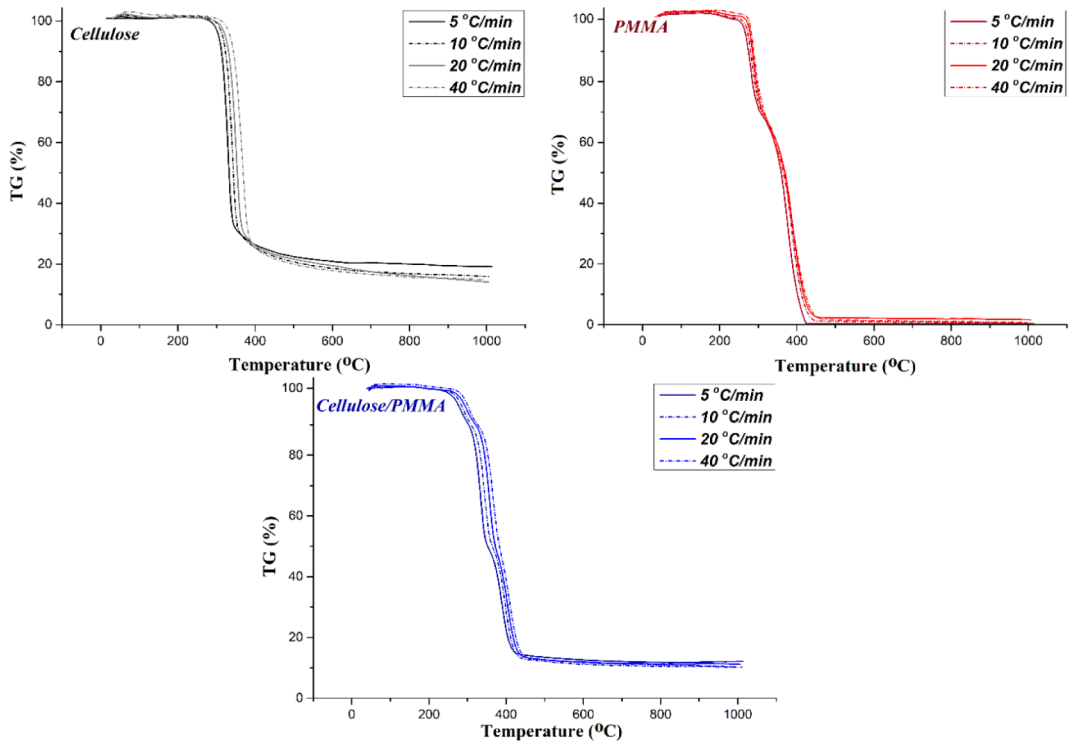

Fig. 1. TG curves of cellulose, PMMA and cellulose/PMMA blend at the different heating rates.

chemical reaction or to produce an activated complex (an intermediate stage between reactants and products) is known as activation energy. In kinetics, lower activation energies point out that higher reaction rates can be attained by providing lower energy. Likewise, for any pre-exponential factor, the higher activation energy values signify that product formation would require more energy to take a start (Shahid et al., 2019). As it may be observed for the results belonging to cellulose, the values of regression coefficients were between 0.9819 and 0.9966 depending on the applied kinetic method and the activation energy distribution were found in accordance apart from the applied method. The activation energy at low conversion gradually decreased up to a conversion degree of 0.8 according to the FWO and KAS models and a

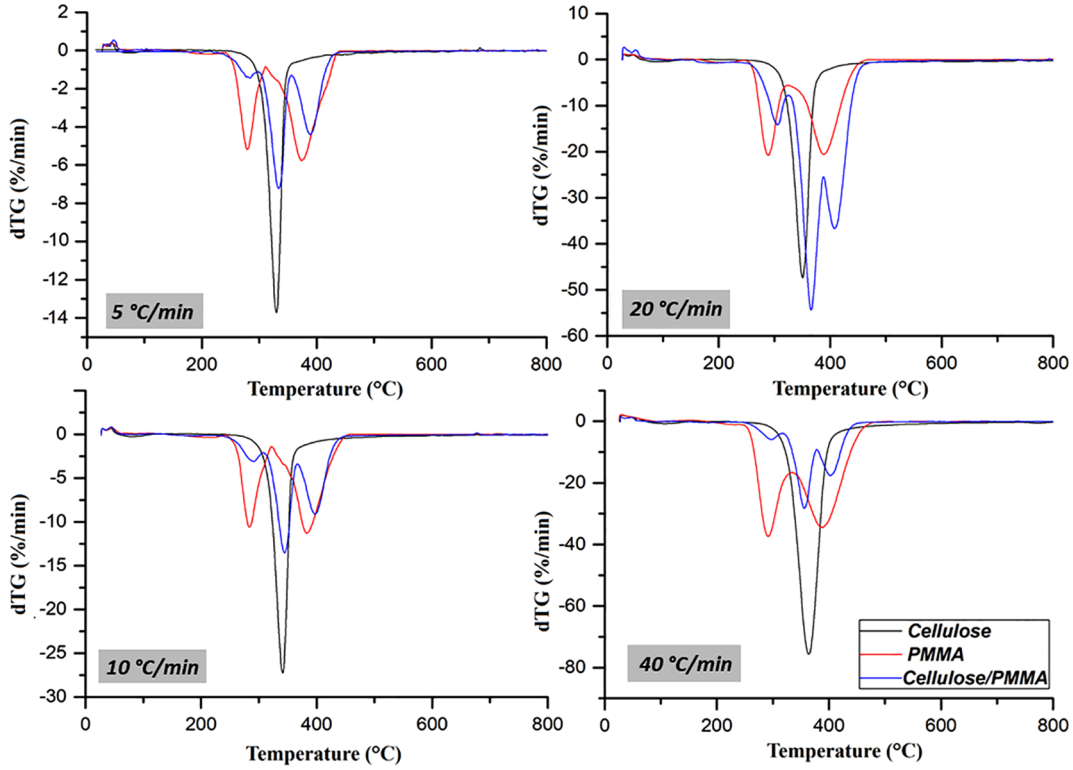

Fig. 2. dTG curves of cellulose, PMMA and cellulose/PMMA blend at the different heating rates.

Table 2
Characteristic pyrolysis temperatures for biomass samples from TG and dTG curves.

Sample	β (°C/min)	T_i (°C)	Tp's (°C)	T_f (°C)	R_p (%/min.mg)
Cellulose	5	263.74	329.98	413.55	1.30
	10	270.25	341.19	427.08	2.78
	20	274.09	350.23	435.96	4.52
	40	276.82	363.70	454.45	7.31
PMMA	5	238.68	297.14; 373.37	437.44	0.49
	10	240.76	284.02; 382.62	455.47	1.01
	20	242.61	288.44; 388.88	466.96	1.95
	40	248.25	291.55; 388.90	476.86	3.38
Cellulose/PMMA (50 wt.%/50 wt%)	5	245.30	283.65; 333.37; 388.21	436.81	0.76
	10	248.88	291.05; 344.42; 397.65	447.65	1.46
	20	251.66	297.21; 356.00; 403.31	460.58	2.94
	40	254.69	305.86; 365.67; 408.05	468.27	5.39
Cellulose/PMMA (75 wt.%/25 wt%)	5	256.72	331.30; 391.50	425.53	0.78
	10	258.29	342.11; 395.79	436.31	1.55
	20	261.85	354.90; 406.71	453.93	2.96
	40	266.54	364.89	466.47	5.41

T_i is the initial active pyrolysis temperature.
Tp's are the peak temperatures in active pyrolysis zone.
T_f is the the terminal active pyrolysis temperature.
Rp is the pyrolysis reactivity.

conversion degree of 0.7 according to the Friedman method. At the last stage of pyrolysis, the activation energy increased slightly. The relatively high activation energy implied higher temperature required to decompose the structure at higher cellulose conversion during pyrolysis. The average values of the activation energy were 164.3, 180.5 and 179.6 kj/mol for the Friedman, FWO and KAS models, respectively.

Dealing with the pyrolysis of PMMA, the activation energy values changed from 414.3 to 786.1 kJ/mol at various conversion degrees depending on the employed model. The regression coefficient for PMMA pyrolysis was in the range of 0.9733 and 0.9984 which signified compatible fitting of the data. The activation energy values of PMMA pyrolysis were fully dependent on the conversion degree in an interval between 0.1 and 0.9. The fluctuations in the values of activation energy were also significant for PMMA degradation. It is inconvenient to interpret the exact reason of activation energy fluctuations in thermal decomposition processes. However, a subtle point to consider is that such variation in activation energy distribution is a result of variation in the reaction mechanism which is practically complex to predict as a general rule of thumb (Salema et al., 2019). Considering the values of the average activation energy by the Friedman method, it may be understood that the mean value for PMMA was 610.7 kJ/mol, which was slightly different than the average activation energies of the other two kinetic methods as FWO and KAS as respectively 613.0 and 622.1 kJ/mol. Although pyrolytic degradation of PMMA started earlier than cellulose, the energy requirement for PMMA was far too much. This may suggest that; cellulosic wastes such as biomass may be

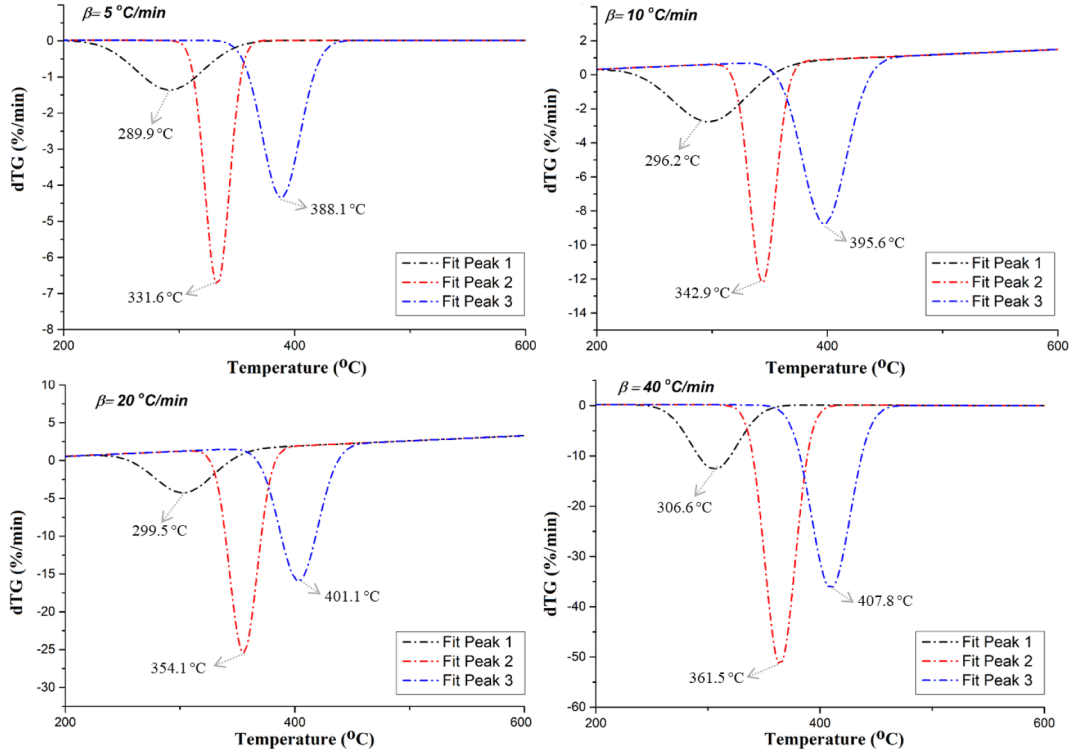

Fig. 3. Deconvoluted dTG curves for co-pyrolysis at the various heating rates.

Table 3
Activation energy with respect to conversion degree for pyrolysis and co-pyrolysis of cellulose and PMMA.

		Friedman		FWO		KAS	
	(α)	E_a (kJ/mol)	R^2	E_a (kJ/mol)	R^2	E_a (kJ/mol)	R^2
Cellulose	0.1	190.2	0.9959	197.8	0.9962	198.2	0.9958
	0.2	181.5	0.9960	191.4	0.9965	191.3	0.9961
	0.3	172.1	0.9960	187.1	0.9967	186.7	0.9963
	0.4	164.6	0.9941	182.9	0.9966	182.2	0.9962
	0.5	159.8	0.9877	178.7	0.9958	177.7	0.9953
	0.6	152.5	0.9819	174.7	0.9948	173.5	0.9940
	0.7	150.8	0.9823	171.4	0.9941	169.9	0.9933
	0.8	152.1	0.9896	168.4	0.9935	166.7	0.9926
	0.9	155.3	0.9851	172.3	0.9948	170.7	0.9941
	Average	164.3	0.9898	180.5	0.9954	179.6	0.9949
PMMA	0.1	509.8	0.9866	414.3	0.9746	426.7	0.9736
	0.2	457.0	0.9908	460.0	0.9846	474.6	0.9841
	0.3	675.7	0.9805	535.4	0.9960	553.6	0.9958
	0.4	742.6	0.9898	644.3	0.9823	667.6	0.9818
	0.5	570.4	0.9917	666.9	0.9870	691.0	0.9867
	0.6	675.3	0.9862	786.1	0.9740	757.1	0.9733
	0.7	645.4	0.9839	724.6	0.9787	748.8	0.9781
	0.8	660.7	0.9984	691.9	0.9864	691.8	0.9859
	0.9	559.5	0.9797	593.5	0.9917	588.1	0.9914
	Average	610.7	0.9875	613.0	0.9839	622.1	0.9834
Cellulose/PMMA (50 wt.%/50 wt%)	0.1	299.2	0.9968	263.7	0.9931	267.8	0.9925
	0.2	190.2	0.9996	204.5	0.9940	205.1	0.9934
	0.3	191.3	0.9967	199.9	0.9953	200.0	0.9948
	0.4	191.4	0.9978	197.4	0.9970	197.3	0.9967
	0.5	188.1	0.9958	193.8	0.9988	193.5	0.9987
	0.6	362.7	0.9999	234.8	0.9997	236.3	0.9996
	0.7	364.3	0.9946	336.3	0.9906	342.8	0.9901
	0.8	351.3	0.9885	347.3	0.9855	354.2	0.9847
	0.9	341.6	0.9943	342.5	0.9906	349.0	0.9901
	Average	275.6	0.9960	257.8	0.9938	260.7	0.9934
Cellulose/PMMA (75 wt.%/25 w t%)	0.1	195.0	0.9860	194.3	0.9982	194.6	0.9980
	0.2	188.0	0.9838	191.4	0.9977	191.3	0.9975
	0.3	170.0	0.9942	186.4	0.9970	185.9	0.9967
	0.4	163.4	0.9899	181.9	0.9968	181.0	0.9964
	0.5	174.2	0.9952	177.5	0.9959	176.3	0.9954
	0.6	165.3	0.9902	173.7	0.9935	172.3	0.9926
	0.7	147.2	0.9807	181.5	0.9852	180.4	0.9835
	0.8	363.2	0.9891	331.2	0.9877	337.5	0.9869
	0.9	223.3	0.9999	241.0	0.9821	242.3	0.9804
	Average	198.8	0.9899	206.5	0.9927	206.8	0.9919

advantageous for decreasing the activation energy of PMMA pyrolysis.

For the co-pyrolysis process of cellulose and PMMA using a blending ratio of 50 wt% cellulose/50 wt% PMMA, the linear fit at different conversion degrees also had fairly high linear correlation coefficients between 0.9847 and 0.9999 depending on the applied kinetic model suggesting that the values of the activation energy satisfied the accuracy of the fitting requirements with the experimental data. The activation energy values tended to decrease up to a conversion degree of 0.5, and then resulted in fluctuations at higher conversion degrees till the end of the active pyrolysis region. A sharp rise in activation energy was observed after a half-conversion of cellulose and PMMA blend. This sharp increase in activation energy may be attributed to the change of reaction chemistry (Mehmood et al., 2019). According to the Friedman model, the activation energy values were between 188.1 and 364.3 kJ/mol with an average value of 275.6 kJ/mol for co-pyrolysis. On the other hand, the mean values of activation energy were 257.8 and 260.7 kj/mol according to the FWO and KAS models, respectively. On the other hand, increasing cellulose quantity during co-pyrolysis up to 75 wt% decreased average activation energy values. The values of co-pyrolysis activation energy by using 75 wt% of cellulose were calculated as 198.8, 206.5 and 206.8 kJ/mol by applying Friedman, FWO and KAS models, respectively. Throughout the whole range of conversion degrees of co-pyrolysis, complex competitive or consecutive multi-step reactions occurred between the radicals which were formed as a result of fragmentation of cellulose and PMMA. All in all, linear relationships were obtained for all of the applied iso-conversional methods for the pyrolysis and co-pyrolysis processes. The values of activation energy at each conversion degree calculated by the FWO and KAS methods were found to be very similar. The deviations between the results of the activation energy were due to the fact that different approximations were used to calculate the temperature integral. Since the Friedman method does not consider the temperature integral, a considerable difference than the other two kinetic methods was observed.

The results of the pre-exponential factor were tabulated in Table 4 to determine pyrolytic and co-pyrolytic potential of cellulose and PMMA together with the favorability and status of the products. The pre-exponential values of PMMA were estimated between 3.19×10^9 and 9.07×10^{12} s^{-1} with an average value of 4.44×10^{11} s^{-1}. On the other hand, much higher pre-exponential factors were calculated during the pyrolysis of PMMA which indicated the intense frequency of the collisions. The collision frequencies of co-pyrolysis experiments using different blending ratios were found between the values that were calculated for the individual components, as expected.

3.3. In-situ evolved gas analysis

In order to extract information in regard to the evolution dynamics of volatiles from the pyrolysis process, the hyphenated TGA/FT-IR technique was used. In order to compare the evolved gases in the fast pyrolysis conditions, the highest heating rate in the study as 40 °C/min

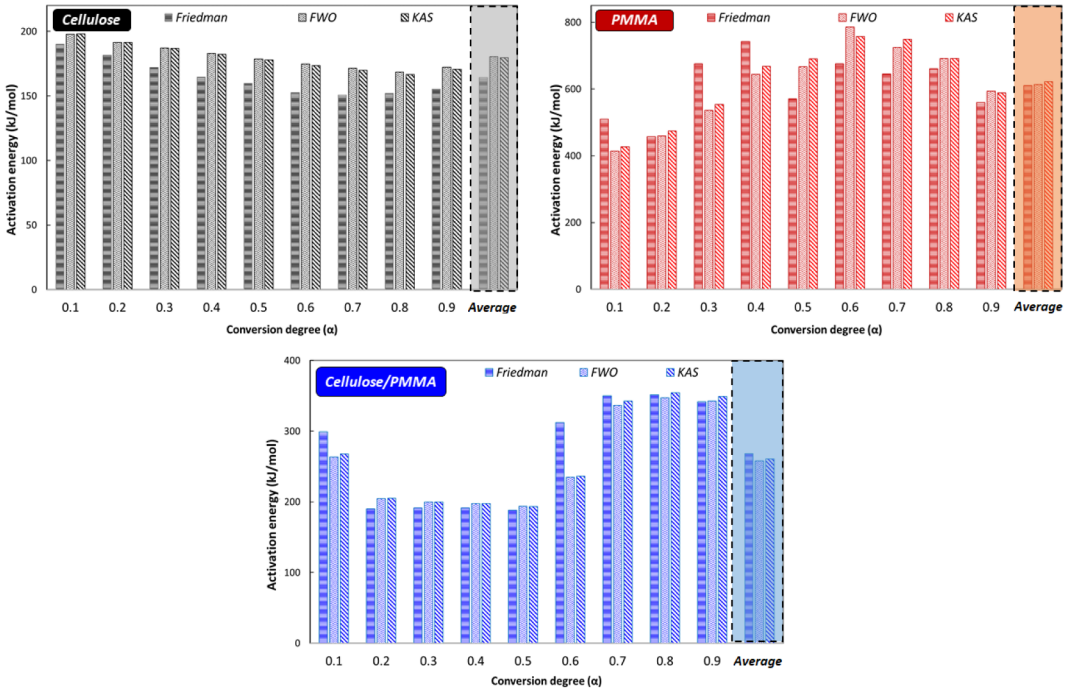

Fig .4. Activation energy as a function of conversion degree for cellulose, PMMA and their blends using Friedman, FWO and KAS methods.

Table 4
Calculated pre-exponential factors for pyrolysis and co-pyrolysis processes (1/s).

α	Cellulose	PMMA	Cellulose/PMMA (50 wt.%/50 wt%)	Cellulose/PMMA (75 wt.%/25 wt%)
0.1	9.07×10^{12}	1.25×10^{45}	1.93×10^{22}	2.23×10^{13}
0.2	1.58×10^{12}	1.25×10^{40}	7.35×10^{12}	5.48×10^{12}
0.3	2.35×10^{11}	5.91×10^{60}	9.22×10^{12}	1.46×10^{11}
0.4	5.19×10^{10}	1.20×10^{67}	9.34×10^{12}	3.86×10^{10}
0.5	1.96×10^{10}	6.62×10^{50}	4.84×10^{12}	3.39×10^{11}
0.6	4.51×10^{9}	5.35×10^{60}	2.43×10^{23}	5.66×10^{10}
0.7	3.19×10^{9}	8.04×10^{57}	4.58×10^{26}	1.48×10^{9}
0.8	4.17×10^{9}	2.26×10^{59}	5.72×10^{26}	7.92×10^{27}
0.9	8.04×10^{9}	6.22×10^{49}	8.42×10^{25}	6.39×10^{15}
Average	4.44×10^{11}	1.34×10^{66}	1.24×10^{26}	8.80×10^{26}

was selected for the evolved gas analysis since slower heating rates cause formation of char in high yields while higher heating rates are used to increase the yields of condensable and non-condensable volatiles. The obtained 3-dimensional (3D) spectra with the instantaneous FT-IR spectra at the maximum peak temperature during pyrolysis and co-pyrolysis processes are important to monitor evolved gasses.

It is known that active cellulose is formed at the initial stage of cellulose pyrolysis, and then, active cellulose is converted to levoglucosan by depolymerization and is reacted to form anhydrocellulose by dehydration. These two competing depolymerization and dehydration reactions are believed to continue the further heterogeneous reaction pathways, which yield gaseous, liquid and solid products (Matsuzawa et al., 2001). As it may be seen in the spectrum, the characteristic peaks between 2250 and 2500 cm^{-1} and bending vibrations between 580 and 730 cm^{-1} of stretching vibrations indicated evolution of carbon dioxide at a higher rate during pyrolysis of cellulose. Additionally, the slight vibrations between 2200 and 2000 cm^{-1} showed removal of carbon monoxide from the cellulosic matrix. These carbon dioxide and carbon monoxide evolution from the structure were mainly due to fragmentation and secondary reactions. Furthermore, O–H peak which were located between 3100 and 3500 cm^{-1} in the spectra belonging split of water due to intermolecular and intramolecular dehydration reactions. It is known that intermolecular dehydration reactions lead to formation of additional covalent bonds, resulting in a higher reticulation and an enhanced thermal stability of the structure. On the other hand, intramolecular dehydration causes formation of C=C double bonds, which may further contribute to aromatization of the structure by formation of benzene rings composing the structure of char (Collard & Blin, 2014). Evolution of high amounts of carbon dioxide and water vapor was also agreed upon with previous thermal degradation studies performed with cellulose (Matsuzawa et al., 2001). Other than these three gases, hundreds of volatile species such as anhydrosugars and their derivatives, furans, acids, aldehydes, light linear carbonyls and oxygenates (Lu et al., 2011; Mettler et al., 2012; Wang et al., 2018) are known to be evolved during the pyrolytic decomposition process of cellulose since cellulose degradation is regarded as a complicated process among researchers. Similar evolved gases were also observed in the pyrolysis of different biomass species including corncob (Wang et al., 2010), pea waste(Müsellim et al., 2018), bamboo(Chen et al., 2015), palm kernel shell (Ma et al., 2015), wheat straw(Lazdovica et al., 2015), spruce and pine wood chips (Salema et al., 2014) due to the high cellulose contents of the samples. Differences in evolution profiles of the gasses may be attributed to the relative proportions of the cellulose, hemicellulose, and lignin together with minor extractives and inorganics.

During PMMA pyrolysis, both 3D and instantaneous FT-IR indicated depolymerization of PMMA, which results in formation of the methyl methacrylate monomer. The peak near 2970 cm^{-1} of methyl ($–CH_3$) and methylene ($–CH_2$) stretching vibrations and the peak near 1750 cm^{-1} assigned to carbonyl (C=O) absorption vibration were specified for methyl methacrylate. Moreover, the stretching vibration of C–O was located at about 1170 cm^{-1}. The peaks around 1450 cm^{-1} and 1310 cm^{-1} were also ascribed to the bending vibrations of $–CH_2$ and $–CH_3$. Additionally, the peaks between 2250 and 2500 cm^{-1} and 580 and 730 cm^{-1} showed evolution of carbon dioxide as it was observed in cellulose degradation. It may be observed that the evolution profile of the co-pyrolysis process was more complicated than that of pyrolysis of cellulose and PMMA since it exhibited a wide range of peaks corresponding to different functional groups and their overlapping peaks. Although new peaks were not observed in the

instantaneous spectra for the co-pyrolysis process, the evolution profiles were slightly changed due to overlapping.

3.4. SEM-EDX and FT-IR analysis of the solid residues

Functional groups, elemental composition and morphology of the residues during several stages of co-pyrolysis were analyzed in order to gain more information about the decomposition mechanism. The surface morphology of the samples at different temperature stages was investigated using SEM-EDX technique. For all of the solid intermediates and the products, cracks and voids on the surface were formed and fragmented surfaces were occurred due to the gas evolution during pyrolytic and co-pyrolytic decomposition. These structures may be deduced to devolatilization, cracking and shrinking of the precursors. Also, the formation of the free radicals might react on the surface, which further causes disintegration of the solid matrix, thus forming an irregular fragmented surface. It can be seen that PMMA blending to cellulose has an influence on the surface morphology and elemental composition of the solid products. In addition, smaller fragments and some pores appear around the larger fragments when the temperature rises to 500 °C during co-pyrolysis. The EDX analysis results showed that the contents of C and O for cellulose char were 85.54 and 14.46 wt %, respectively at 500 °C. On the other hand, cellulose/PMMA co-pyrolytic char had C and O contents as 84.41 and 15.59 wt% at this temperature which indicated that blending PMMA slightly enriched oxygen content of the solid product during co-pyrolysis. When the effect of temperature on co-pyrolytic solid residues was examined, a stepwise increment in the carbon content from 48.58 to 49.2 wt% was noticeable from 300 to 400 °C. However, when the temperature was raised to 500 °C, a sharp increase in the carbon content from 49.2 to 84.41was noticeable. This may be attributed to the densification of deoxygenation reactions between 400 and 500 °C during co-pyrolysis. Changes in the morphology and elemental composition are also confirmed by EDX mapping was done for evaluation of the chemical composition by a semi-quantitative analysis of the elemental distribution of the solid product microdomains.

Intermediate solid residues at different temperature stages during pyrolysis and char at the end of the active pyrolysis region were also analyzed by FT-IR spectroscopy. According to the results, increasing co-pyrolysis temperature from 300 to 500 °C led to the elimination of hydroxyl groups from the solid matrix which may be observed from O-H stretching vibration between 3100 and 3500 cm^{-1}. Besides, both cellulose char and co-pyrolytic char obtained at 500 °C had peaks near 1595 cm^{-1} which is assigned to aromatic C=C stretching. Intensities of C–H stretching band near 2970 cm^{-1} shows the presence of aliphatic groups on co-pyrolytic char and effect of temperature due to the elimination of side groups of PMMA structure. On the other hand, stretching around 1720 cm^{-1} in the spectra of co-pyrolytic chars indicates that C=O groups which is not observed on cellulose char.

4. Conclusions

The pyrolysis of cellulose was a single-stage degradation where most of the thermal transformation occurs between 263.74 and 454.45 °C while multi-stage pyrolytic degradation stage of PMMA happened between 238.68 and 476.86 °C. Based on the iso-conversional approach, the strikingly good prediction for cellulose and PMMA pyrolysis together with co-pyrolysis was demonstrated. Activation energy of PMMA was reduced by blending cellulose which may trigger complex competitive or consecutive multi-step reactions. Also, a large variety of chemical species was identified by simultaneous TGA/FT-IR system. The results of this study may promote the advancement of future co-pyrolysis studies of cellulosic precursors with PMMA.

Author contribution

Dr. Gamzenur ÖZSİN conceived of the presented idea, conducted the overall experiments, analyzed the data, interpreted the results, wrote original draft and edited the manuscript.

Acknowledgements

The author thanks to the Carbon Materials Processing Group of Eskişehir Technical University, Department of Chemical Engineering for facilitating TGA/FT-IR experiments.

Appendix A. Supplementary data

Supplementary data to this article can be found online at https://doi.org/10.1016/j.biortech.2019.122700.

References

Jin, Q., Wang, X., Li, S., Mikulčić, H., Bešenić, T., Deng, S., Vujanović, M., Tan, H., Kumfer, B.M., 2017. Synergistic effects during co-pyrolysis of biomass and plastic: Gas, tar, soot, char products and thermogravimetric study. J. Energy Inst. 92 (1), 108–117.
Singhania, R.R., Patel, A.K., Sukumaran, R.K., Larroche, C., Pandey, A., 2013. Role and significance of beta-glucosidases in the hydrolysis of cellulose for bioethanol production. Bioresour. Technol. 127, 500–507.
Cherpozat, L., Loranger, E., Daneault, C., 2019. Ultrasonic pretreatment of soft wood biomass prior to conventional pyrolysis: Scale-up effects and limitations. Biomass Bioenergy. 124, 54–63.
Sharifzadeh, M., Richard, C., Liu, K., Hellgardt, K., Chadwick, D., Shah, N., 2015. An integrated process for biomass pyrolysis oil upgrading: A synergistic approach. Biomass Bioenergy. 76, 108–117.
Awasthi, A., Singh, G., Dhyani, V., Kumar, J., Reddy, Y.S., Adarsh, V., Puthiyamadam, A., Mullepureddy, K.K., Sukumaran, R.K., Ummalyma, S.B., 2019. Co-pyrolysis of Phumdi and Para grass biomass from Loktak Lake. Bioresour. Technol. 285, 121308.
Chen, R., Zhang, J., Lun, L., Li, Q., Zhang, Y., 2019. Comparative study on synergistic effects in co-pyrolysis of tobacco stalk with polymer wastes: Thermal behavior, gas formation, and kinetics. Bioresour. Technol. 292, 121970.
Ding, K., He, A., Zhong, D., Fan, L., Liu, S., Wang, Y., Liu, Y., Chen, P., Lei, H., Ruan, R., 2018. Improving hydrocarbon yield via catalytic fast co-pyrolysis of biomass and plastic over ceria and HZSM-5: An analytical pyrolyzer analysis. Bioresour. Technol. 268, 1–8.
Bartocci, P., Bidini, G., Asdrubali, F., Beatrice, C., Frusteri, F., Fantozzi, F., 2018. Batch pyrolysis of pellet made of biomass and crude glycerol: mass and energy balances. Renew. Energy. 124, 172–179.
Déparrois, N., Singh, P., Burra, K., Gupta, A., 2019. Syngas production from co-pyrolysis and co-gasification of polystyrene and paper with CO_2. Appl. Energy. 246, 1–10.
Jin, X., Chen-yang, N., Deng-yin, Z., Yan-hui, G., Qi-min, H., Yu-hong, X., 2019. Co-pyrolysis of rice straw and water hyacinth: Characterization of products, yields and biomass interaction effect. Biomass Bioenergy. 127, 105281.
Patil, V., Adhikari, S., Cross, P., 2018. Co-pyrolysis of lignin and plastics using red clay as catalyst in a micro-pyrolyzer. Bioresour. Technol. 270, 311–319.
Li, X., Zhang, H., Li, J., Su, L., Zuo, J., Komarneni, S., Wang, Y., 2013. Improving the aromatic production in catalytic fast pyrolysis of cellulose by co-feeding low-density polyethylene. Appl. Catal. A-Gen. 455, 114–121.
Xiang, Z., Liang, J., Morgan Jr, H.M., Liu, Y., Mao, H., Bu, Q., 2018. Thermal behavior and kinetic study for co-pyrolysis of lignocellulosic biomass with polyethylene over Cobalt modified ZSM-5 catalyst by thermogravimetric analysis. Bioresour. Technol. 247, 804–811.
Kumari, N., Singh, R., 2019. Co-pyrolysis of waste Polypropylene and Rice bran wax-Production of biofuel and its characterization. J. Energy Inst. 92 (4), 933–946.
Salema, A.A., Afzal, M.T., Motasemi, F., 2014. Is there synergy between carbonaceous material and biomass during conventional pyrolysis? A TG-FTIR approach. J. Anal. Appl. Pyrolysis. 105, 217–226.
Yang, H., Yan, R., Chen, H., Lee, D.H., Zheng, C., 2007. Characteristics of hemicellulose, cellulose and lignin pyrolysis. Fuel 86, 1781–1788.
Yang, H., Yan, R., Chen, H., Zheng, C., Lee, D.H., Liang, D.T., 2006. In-depth investigation of biomass pyrolysis based on three major components: hemicellulose, cellulose and lignin. Energ. Fuel. 20 (1), 388–393.
Collard, F.-X., Blin, J., 2014. A review on pyrolysis of biomass constituents: Mechanisms and composition of the products obtained from the conversion of cellulose, hemicelluloses and lignin. Renew. Sust. Energ. Rev. 38, 594–608.
Stefanidis, S.D., Kalogiannis, K.G., Iliopoulou, E.F., Michailof, C.M., Pilavachi, P.A., Lappas, A.A., 2014. A study of lignocellulosic biomass pyrolysis via the pyrolysis of cellulose, hemicellulose and lignin. J. Anal. Appl. Pyrolysis. 105, 143–150.
Burhenne, L., Messmer, J., Aicher, T., Laborie, M.-P., 2013. The effect of the biomass components lignin, cellulose and hemicellulose on TGA and fixed bed pyrolysis. J. Anal. Appl. Pyrolysis. 101, 177–184.
Zhang, J., Choi, Y.S., Yoo, C.G., Kim, T.H., Brown, R.C., Shanks, B.H., 2015. Cellulose–hemicellulose and cellulose–lignin interactions during fast pyrolysis. ACS

Sustain. Chem. Eng. 3 (2), 293–301.
Qu, T., Guo, W., Shen, L., Xiao, J., Zhao, K., 2011. Experimental study of biomass pyrolysis based on three major components: hemicellulose, cellulose, and lignin. Ind. Eng. Chem. Res. 50 (18), 10424–10433.
Giudicianni, P., Cardone, G., Ragucci, R., 2013. Cellulose, hemicellulose and lignin slow steam pyrolysis: Thermal decomposition of biomass components mixtures. J. Anal. Appl. Pyrolysis. 100, 213–222.
Zhao, C., Jiang, E., Chen, A., 2017. Volatile production from pyrolysis of cellulose, hemicellulose and lignin. J. Energy Inst. 90 (6), 902–913.
Zhou, H., Long, Y., Meng, A., Chen, S., Li, Q., Zhang, Y., 2015. A novel method for kinetics analysis of pyrolysis of hemicellulose, cellulose, and lignin in TGA and macro-TGA. RSC Adv. 5 (34), 26509–26516.
Bu, Q., Chen, K., Xie, W., Liu, Y., Cao, M., Kong, X., Chu, Q., Mao, H., 2019. Hydrocarbon rich bio-oil production, thermal behavior analysis and kinetic study of microwave-assisted co-pyrolysis of microwave-torrefied lignin with low density polyethylene. Bioresour. Technol. 291, 121860.
Shafaghat, H., Lee, H.W., Tsang, Y.F., Oh, D., Jae, J., Jung, S.-C., Ko, C.H., Lam, S.S., Park, Y.-K., 2019. In-situ and ex-situ catalytic pyrolysis/co-pyrolysis of empty fruit bunches using mesostructured aluminosilicate catalysts. Chem. Eng. J. 366, 330–338.
Debiagi, P.E.A., Gentile, G., Pelucchi, M., Frassoldati, A., Cuoci, A., Faravelli, T., Ranzi, E., 2016. Detailed kinetic mechanism of gas-phase reactions of volatiles released from biomass pyrolysis. Biomass Bioenergy 93, 60–71.
Matsuzawa, Y., Ayabe, M., Nishino, J., 2001. Acceleration of cellulose co-pyrolysis with polymer. Polym. Degrad. Stabil. 71 (3), 435–444.
Suriapparao, D.V., Ojha, D.K., Ray, T., Vinu, R., 2014. Kinetic analysis of co-pyrolysis of cellulose and polypropylene. J. Thermal Anal. Calorim. 117 (3), 1441–1451.
Tahir, M.H., Zhao, Z., Ren, J., Rasool, T., Naqvi, S.R., 2019. Thermo-kinetics and gaseous product analysis of banana peel pyrolysis for its bioenergy potential. Biomass Bioenergy 122, 193–201.
Yan, J., Jiao, H., Li, Z., Lei, Z., Wang, Z., Ren, S., Shui, H., Kang, S., Yan, H., Pan, C., 2019. Kinetic analysis and modeling of coal pyrolysis with model-free methods. Fuel 241, 382–391.
Amini, E., Safdari, M.-S., Weise, D.R., Fletcher, T.H., 2019. Pyrolysis kinetics of live and dead wildland vegetation from the Southern United States. J. Anal. Appl. Pyrol. 142, 104613.
Ashraf, A., Sattar, H., Munir, S., 2019. A comparative applicability study of model-fitting and model-free kinetic analysis approaches to non-isothermal pyrolysis of coal and agricultural residues. Fuel 240, 326–333.
Bedoić, R., Bulatović, V.O., Čuček, L., Ćosić, B., Špehar, A., Pukšec, T., Duić, N., 2019. A kinetic study of roadside grass pyrolysis and digestate from anaerobic mono-digestion. Bioresour. Technol. 292, 121935.
Wilkie, C.A., 1999. TGA/FTIR: an extremely useful technique for studying polymer degradation. Polym. Degrad. Stabil. 66 (3), 301–306.
Laachachi, A., Cochez, M., Ferriol, M., Leroy, E., Cuesta, J.L., Oget, N., 2004. Influence of Sb_2O_3 particles as filler on the thermal stability and flammability properties of poly (methyl methacrylate)(PMMA). Polym. Degrad. Stabil. 85 (1), 641–646.
Shahid, A., Ishfaq, M., Ahmad, M.S., Malik, S., Farooq, M., Hui, Z., Batawi, A.H., Shafi, M.E., Aloqbi, A.A., Gull, M., 2019. Bioenergy potential of the residual microalgal biomass produced in city wastewater assessed through pyrolysis, kinetics and thermodynamics study to design algal biorefinery. Bioresour. Technol. 289, 121701.
Salema, A.A., Ting, R.M.W., Shang, Y.K., 2019. Pyrolysis of blend (oil palm biomass and sawdust) biomass using TG-MS. Bioresour. Technol. 274, 439–446.
Mehmood, M.A., Ahmad, M.S., Liu, Q., Liu, C.-G., Tahir, M.H., Aloqbi, A.A., Tarbiah, N.I., Alsufiani, H.M., Gull, M., 2019. Helianthus tuberosus as a promising feedstock for bioenergy and chemicals appraised through pyrolysis, kinetics, and TG-FTIR-MS based study. Energy Convers. Manag. 194, 37–45.
Wang, W., Wang, M., Huang, J., Tang, N., Dang, Z., Shi, Y., Zhaohe, M., 2018. Microwave-assisted catalytic pyrolysis of cellulose for phenol-rich bio-oil production. J. Energy Inst. 92 (6), 1997–2003.
Mettler, M.S., Mushrif, S.H., Paulsen, A.D., Javadekar, A.D., Vlachos, D.G., Dauenhauer, P.J., 2012. Revealing pyrolysis chemistry for biofuels production: Conversion of cellulose to furans and small oxygenates. Energ. Environ. Sci. 5 (1), 5414–5424.
Lu, Q., Yang, X.-C., Dong, C.-Q., Zhang, Z.-F., Zhang, X.-M., Zhu, X.-F., 2011. Influence of pyrolysis temperature and time on the cellulose fast pyrolysis products: Analytical Py-GC/MS study. J. Anal. Appl. Pyrolysis. 92 (2), 430–438.
Wang, D., Xiao, R., Zhang, H., He, G., 2010. Comparison of catalytic pyrolysis of biomass with MCM-41 and CaO catalysts by using TGA–FTIR analysis. J. Anal. Appl. Pyrolysis. 89 (2), 171–177.
Müsellim, E., Tahir, M.H., Ahmad, M.S., Ceylan, S., 2018. Thermokinetic and TG/DSC-FTIR study of pea waste biomass pyrolysis. Appl. Therm. Eng. 137, 54–61.
Chen, D., Liu, D., Zhang, H., Chen, Y., Li, Q., 2015. Bamboo pyrolysis using TG–FTIR and a lab-scale reactor: Analysis of pyrolysis behavior, product properties, and carbon and energy yields. Fuel. 148, 79–86.
Ma, Z., Chen, D., Gu, J., Bao, B., Zhang, Q., 2015. Determination of pyrolysis characteristics and kinetics of palm kernel shell using TGA–FTIR and model-free integral methods. Energy Convers. Manag. 89, 251–259.
Lazdovica, K., Liepina, L., Kampars, V., 2015. Comparative wheat straw catalytic pyrolysis in the presence of zeolites, Pt/C, and Pd/C by using TGA-FTIR method. Fuel Process. Technol. 138, 645–653.